MODELING ABLATION OF FIBROUS MATERIALS FROM BULK TO KNUDSEN REGIME

Jean Lachaud and Nagi N. Mansour

NASA Ames Research Center, MS 230-3, Moffett Field, CA 94035, USA

ABSTRACT

Material-environment interactions are analyzed at microscopic scale to explain the lower than expected density observed by post-flight analysis of the char layer on the Stardust shield. Mass transfer, ablation (oxidation), and surface recession of fibrous material is simulated in 3D using a Monte-Carlo simulation tool. Ablation is found to occur either at the surface or in volume depending on Knudsen and Thiele number values. This study supports the idea of volume ablation followed by possible carbon fiber spallation that may explain post-flight analyses.

INTRODUCTION

Thermal protection systems (TPS) of planetary probes are exposed to extreme heat fluxes during atmospheric entry. The latest generation of TPS materials is fabricated by partial impregnation of carbon felt in phenolic resin. The material upper layer (typically 1 cm), exposed to temperatures higher than 1200 K, is pyrolyzed into char. During pyrolysis, the phenolic resin loses up to 50% of its mass, shrinks and weakens. The pyrolyzed resin quickly oxidizes and may spall, revealing the structure of the felt. The felt can be described as a stack of carbon fibers randomly oriented (figure 1). The exposed carbon fibers progressively gasify by oxidation. This leads to mass loss of the carbon structure and wall recession called ablation. This work aims to improve the understanding of this latter process.

Current models describe gasification of the char layer in terms of recession velocity (ablation velocity) of the overall surface. This description, based on models of previous generation TPS materials, has been shown to be correct for low porosity materials [Moyer, 1968]. However, the average surface may not recede uniformly in very porous materials (as in figure 3), but the individual fibers may progressively vanish (as in figure 4) when oxidant penetration inside the porous material is fast enough compared to oxidant consumption by the fibers. In the second regime, ablation is no longer a surface phenomenon, but is volumetric. Seen from a surface point of view, two important consequences follow this volume ablation regime: (1) the effective reactivity of the material is significantly increased; (2) the material weakens in volume and the carbon fibers of the TPS material may be subject to mechanical erosion called spallation. In this context, the objective of this work is to understand when volume ablation may occur in order to determine whether spallation may have occurred during Stardust re-entry and to anticipate any spallation in future missions.

As a first step in modeling volume ablation, this paper considers mass transfer and heterogeneous reaction coupling in random fibrous structure. An important point regarding mass transport during atmospheric entry is that wall pressure varies with atmospheric density and entry velocity. Hence, the molecular mean free path spans many orders of magnitude during entry leading to a wide span of the ablation regimes, successively, from Knudsen, to transition, and finally to bulk diffusion dominated mechanisms.

Fig.1. Post-flight scanning electron microscopy micrograph of Stardust TPS surface [Stackpoole, 2008].

ORGANIZATION

A phenomenological model for volume ablation is proposed. Three-dimensional (3D) numerical simulations of isothermal ablation in air of a carbon felt are performed and analyzed. To guide the analysis, a macroscopic model for volume ablation is derived analytically using volume averaging. The effective diffusivities needed to close the model are computed in bulk diffusion, transition and Knudsen regimes in porous media using direct numerical simulations. The model is used to provide understanding of the post-flight analysis of Stardust observations.

MODEL

Because the aim of this study is to improve the understanding of the char behavior, the focus is set on the material itself. Close to the wall, the velocity of the external airflow is null (no-slip condition); therefore mass transport can be considered diffusive. Knowledge of the value of the intensive variables at the wall (pressure, temperature, gas composition) is sufficient to simulate the material behavior.

Carbon-based TPS is expected to ablate in air at a wall temperature T_w around 3000K. We focus on the char layer that we assume to be composed of carbon fibers only, and that it ablates by oxidation. The layer is assumed to ablate along z, the normal direction, and is considered infinite in x and y directions (see Fig. 2). To start, the temperature of

the sample is assumed homogeneous and steady. In addition, blowing of pyrolysis gases is negligible. The structure of the carbon fibers is assumed homogeneous and isotropic. Finally, we assume heterogeneous oxidation reaction where carbon is consumed that leads to reduction of fiber radius. The motion of the interface between fiber and surrounding fluid can be interpreted as an advancing front with a normal velocity proportional to the oxidation rate [Lachaud. 2008].

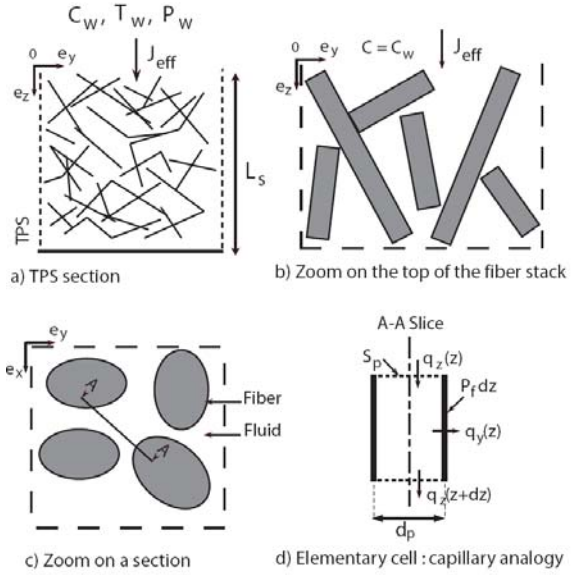

Fig.2. Multi-scale sketches of the computational cell

The interface is represented by a surface function S(x,y,z,t) first order differentiable almost everywhere with constant value (zero) at the interface [Katardjiev, 1994]. The function S satisfies the differential equation:

$$\frac{\partial S}{\partial t} + \vec{v}.\nabla S = 0 \qquad (1)$$

where,

$$\vec{v} = \Omega \cdot J \cdot \vec{n} \qquad (2)$$

is the local surface velocity, with Ω the solid molar volume, J the molar rate of oxidation, and $\vec{n} = \nabla S / \| \nabla S \|$ the normal pointing outwards from the surface. For a first order heterogeneous reaction, the local impinging molar flux density (on a fiber elementary surface) is given by:

$$J = k_f C \qquad (3)$$

with k_f the fiber intrinsic reactivity and C=C(x,y,z,t) the oxygen concentration. The local oxygen consumption is then coupled to the fiber surface recession and mass transfer into the porous medium. Mass transfer of oxygen in air is modeled by binary diffusion. Combining Fick's law and mass conservation, oxygen transport writes:

$$\frac{\partial C}{\partial t} + \nabla \cdot (-D \nabla C) = 0 \qquad (4)$$

The boundary conditions are:

- top (z=0): $C = C_w$ (Dirichlet),
- bottom (z=Ls): $\nabla C = 0$ (Neumann),
- sides: periodic.

For simple material architectures, this model can be solved analytically [Lachaud, 2008]. In the case of random fibrous media, direct numerical simulation or homogenization (averaging) methods are required. These solution methods are summarized in the two following sections.

3D DIRECT NUMERICAL SIMULATION

The fibers distribution at initial time is shown in the first pictures of Fig. 3 and 4. The computational domain is divided into the white part representing the fluid close to the wall and in the porous medium part, the fibers are represented by the black part. The porous medium is represented on a Cartesian grid in a cube of 100^3 voxels (3D pixels). Using a Monte Carlo algorithm, fibers with random positions and orientations are positioned in the cube until the porosity reaches the target value of 0.85. To reproduce realistically the material architecture, fibers are non-overlapping and their direction is azimuthally biased so that they are almost parallel to the topsurface (+/- 15°).

The 3-D time-dependent solution to the reaction/diffusion models described above is obtained using an efficient numerical simulation code, named AMA. The code developed in previous work [Lachaud, 2006], uses Monte-Carlo random walk whose ensemble averaged solution is represented by Eqs. 1 and 4. AMA is a C ANSI implementation with four main features: (a) A 3-D image (graph) containing several phases (fluid and solid in the present case) is described by the discrete cubic voxels method on a Cartesian grid. (b) The moving fluid/solid interfaces are determined by a simplified marching cube approximation (Eq. 1). (c) Mass transfer by diffusion (Eq. 4) is simulated by a random walk using Maxwell-Boltzmann distribution for the velocity in the Knudsen and transition regimes, and a Brownian motion simulation technique in the bulk diffusion regime [Lachaud, 2006]. Brownian motion is a grid-free method that efficiently converges when simulating diffusion in a continuous fluid [Plapp, 2000]. (d) Heterogeneous first-order reaction on the wall (Eq. 3) is simulated by using a sticking probability. Dirichlet boundary condition is handled using a buffer where the concentration of walker is kept constant.

Two simulations carried out in bulk diffusion regime are shown in this paper (Fig. 3 and 4). The material behavior is found to depend on diffusion

velocity to oxidant consumption rate ratio inside the porous medium. When the reaction process is fast compared to mass transfer, the oxidant is mostly consumed at the surface and cannot seep into the porous medium; in this case ablation is a surface phenomenon (Fig. 3). In the converse case, the oxidant consumption being slow, the oxidant concentration becomes homogeneous in the porous medium and ablation occurs in volume (Fig. 4). This volume ablation obviously weakens the structure of the material, which is then likely to undergo spallation under the shear stress of the entry flow. At this point, an analytical study seems useful in order to find the relevant dimensionless number(s) for the involved coupling.

ANALYTICAL SOLUTION (VOLUME AVERAGING)

The behavior of the sample is analyzed at initial time, before ablation has significantly reduced the fiber diameter.

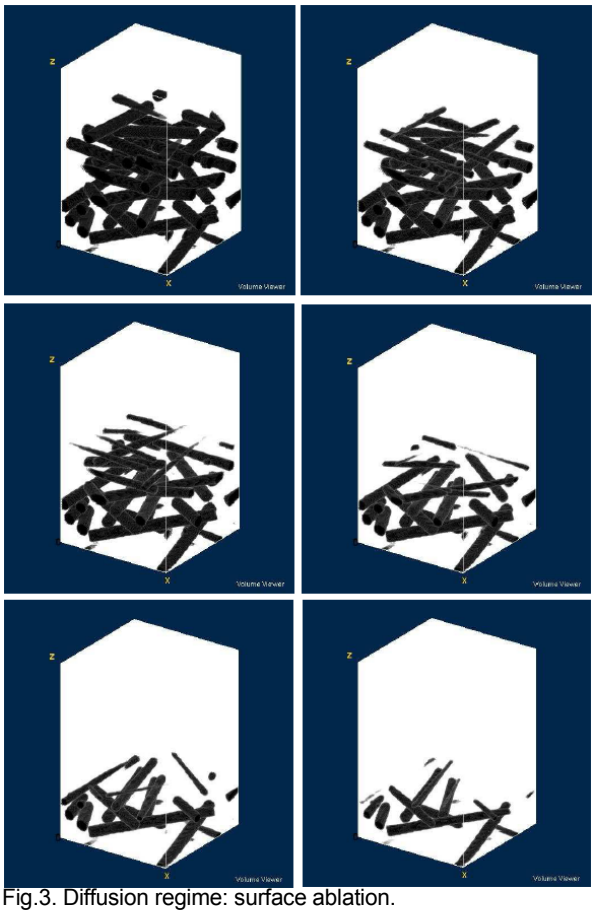

Fig.3. Diffusion regime: surface ablation.

In the literature, porous media are described in terms of mean pore size d_p, porosity ε, volume surface s, and tortuosity η. Assuming cylindrical fibers, the mean pore size writes [Transvalidou, 1996]:

$$d_p = \frac{4\varepsilon}{s} \qquad (5)$$

For the material of interest in this study, d_p is around 50 μm. For mean free paths lower than 1 µm Knudsen number ($Kn=\lambda/d_p$) can be considered low and the regime continuous. In the validity domain of Maxwell-Boltzmann distribution, the mean free path of oxygen in air can be estimated using the following equation [Reid, 1987]:

$$\bar{\lambda} = 95 \cdot 10^{-9} \cdot \frac{10^5 \cdot T}{298 \cdot P} \qquad (6)$$

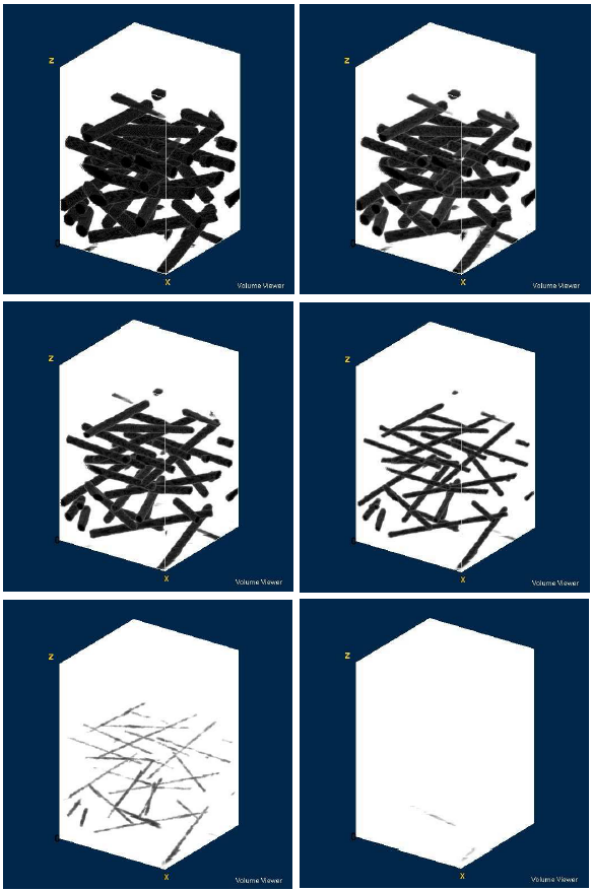

Fig.4. Reaction regime: volume ablation.

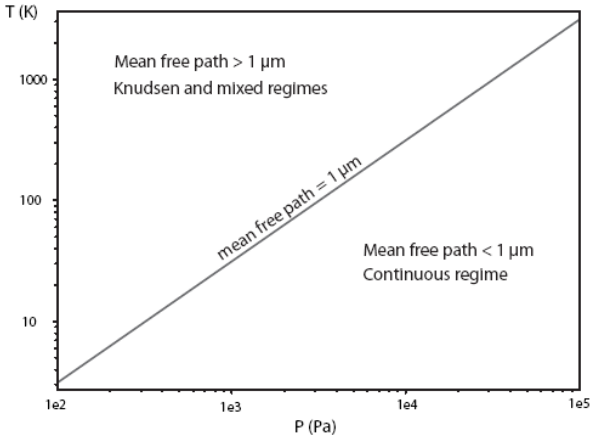

Fig.4. Validity domain of the continuous regime hypothesis.

The temperature/pressure conditions for the validity of the continuous regime hypothesis are plotted in Fig. 4. Outside the validity domain, the mean free path is significantly lowered by gas collisions on the porous material walls. It results in a slower diffusive transport. Fick's law can be homogenized in all regimes. After homogenization in isotropic porous media, the law keeps the same form, but the effective diffusion coefficient writes [Tomadakis, 1993]:

$$D_{eff} = \frac{\varepsilon}{\eta} D_{ref} \qquad (7)$$

D_{ref} is a reference diffusivity, corresponding to the longitudinal diffusivity into a capillary of diameter d_p, which according to Bosanquet's relation writes:

$$\frac{1}{D_{ref}} = \frac{1}{D_B} + \frac{1}{D_K} = \frac{1}{\frac{1}{3}\bar{v}\bar{\lambda}} + \frac{1}{\frac{1}{3}\bar{v}d_p} \qquad (8)$$

with $\bar{v}$ the mean velocity of the molecules (molecular agitation) and $\bar{\lambda}$ the mean free path. The tortuosity η, which is a geometric factor that characterizes the difference between a straight capillary and the actual tortuous medium as far as molecule trajectories are concerned, must be assessed numerically in the general case.

Considering a first order heterogeneous reaction, the local impinging molar flux density (in an equivalent pore) is given by:

$$q_y(z) = k_f C(z) \qquad (9)$$

with C(z) the oxygen concentration at depth *z* (see Fig. 3-d). The mass balance in the elementary cell represented in figures 1-c and 1-d writes [Lachaud, 2007]:

$$q_z(z) - q_z(z+dz) = q_y(z) \qquad (10)$$

$$-D\nabla(C(z) - C(z+dz))S_p = k_f C(z) P_f dz \qquad (11)$$

where D is the local diffusion coefficient ($D = D_{ref}/\eta$), P_f is the local fiber perimeter, and S_p the local horizontal section of the pore. The integration of the ratio S_p/P_f on a representative horizontal section of the sample gives $S_p/P_f = \varepsilon/s$. In summary, $C(z)$ is given by the following differential equation:

$$\frac{\partial^2 C(z)}{\partial z^2} - \frac{4k_f}{d_p D} C(z) = 0 \qquad (12)$$

After integration, the oxygen concentration inside the porous medium is found to be:

$$C(z) = C_0 \frac{\cosh(\Phi(z/L_s - 1)}{\cosh \Phi} \qquad (13)$$

where

$$\Phi = \frac{Ls}{\sqrt{\frac{d_p D}{4k_f}}} \qquad (14)$$

is the Thiele number. The concentration gradient inside the porous medium is then a function of Thiele number, as shown on figure 5. When Thiele number is small, diffusion is much faster than reaction. In this case, the oxidant concentration inside the porous medium is homogeneous and equal to C_0. Therefore, ablation is a volume phenomenon (Fig. 4). In the converse case (high Thiele number), diffusion is not fast enough to bring the oxidant inside the porous medium; only the top of the sample ablates. In this case, ablation is a surface phenomenon (Fig. 3).

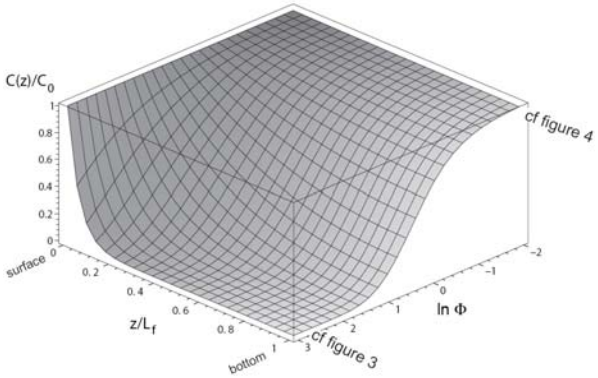

Fig.5. Oxidant concentration inside the porous medium as a function of Thiele number.

In the design of a TPS, knowledge of the effective reactivity k_{eff} of the material is useful. k_{eff} is defined

as the reactivity of a homogeneous, dense and smooth material that would produce the same ablation rate as the porous medium:

$$J_{eff} = C_0 k_{eff} = \int_{z=0}^{L_s} C(z) k_f s dz \qquad (15)$$

The surface of the effective material is placed at abscissa z=0. The ratio of effective to fiber reactivity is obtained by integration of Eq. (15):

$$\frac{k_{eff}}{k_f} = \frac{4\varepsilon L_s}{d_p}\frac{\tanh\phi}{\phi} + (1-\varepsilon) \qquad (16)$$

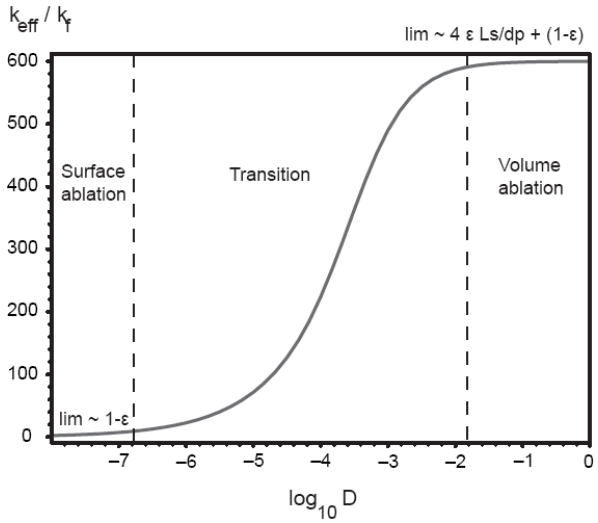

Fig. 6. Normalized effective reactivity as a function of the diffusion coefficient for k_f=1m/s.

As shown in Fig. 6, the material effective reactivity features two limit cases: surface ablation (Fig. 2) and volume ablation (Fig. 3). In the limit cases, the material behavior is no longer a function of the diffusion coefficient, while a strong dependency is observed in the transition regime. In the case of full volume ablation, the effective reactivity is found to be two orders of magnitude higher than the fiber intrinsic reactivity.

EFFECTIVE DIFFUSIVITY (DNS)

In order to apply this model to the analysis of actual problems, the knowledge of the effective diffusion coefficient inside the porous medium represented in figure 7 is required. This material being orthotropic, the diffusion coefficients in x-y and z directions are different. Effective Knudsen, transition, and Bulk diffusion coefficients in a given direction j are obtained through a computer simulation procedure using the mean square displacement in this direction, $\left\langle \xi_j^2 \right\rangle$, after adequately large values of travel time, τ, of a large population of random walkers introduced randomly in the unit cell of the porous medium. The diffusion coefficient in direction j is then obtained using the following relation (Einstein, 1926):

$$D_{e\,j} = \frac{\left\langle \xi_j^2 \right\rangle}{2\tau} \qquad (17)$$

The effective diffusivity inside the porous medium may be assessed for any combination ($\bar{\nu}$, $\bar{\lambda}$). However, equations (7) and (8) show that the only data that cannot be determined analytically is the tortuosity.

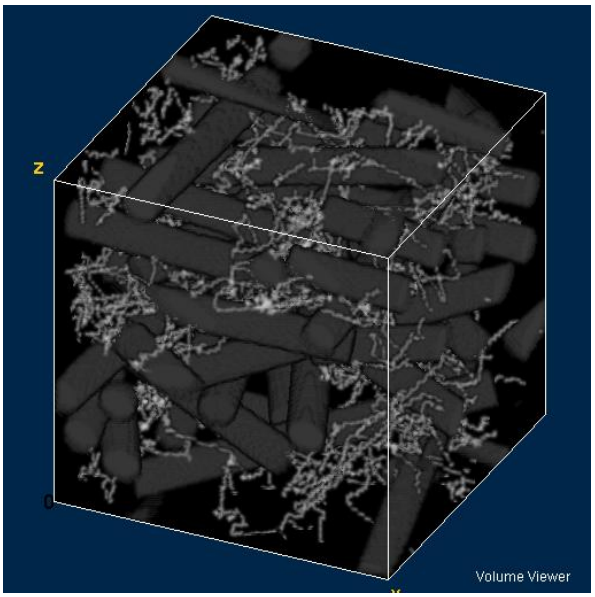

Fig. 7. Path of a random walker (whose mean free path is 5 micrometers) inside the porous medium of the study.

The tortuosity is only a function of $\bar{\lambda}$ and of the porous medium architecture. As a consequence, it is convenient to assess the tortuosity as a function of Knudsen number (figure 8). The simulation tool presented in the first section is used again. In order to assure convergence, the simulations have been carried out with a total number of 10,000 walkers, and for a path one thousand times larger than the elementary cell side. The numerical procedure has been validated for a square array of parallel cylinders in comparison with analytical results [Perrins, 1979] in bulk diffusion regime and with numerical results in transition and Knudsen regime [Tomadakis, 1993; Vignoles, 2007]. Tomadakis and Sotirchos [Tomadakis, 1993] also studied random fiber structures but they were isotopic and with overlapping fibers, so they are not comparable to the anisotropic and non-overlapping fiber structure of this study. The extension of Bosanquet's relation to ordinary porous media by defining a bulk tortuosity (η_B) and a Knudsen tortuosity (η_K) has been shown to provide a good interpolation of numerical data for

random fibrous structures [Tomadakis, 1993]. Under this extension, the effective tortuosity writes:

$$\eta = \frac{\eta_B + \eta_K Kn}{1 + Kn} \tag{18}$$

The curves of figure 7 have been plotted using this approximation. A correct interpolation is obtained again for non-overlapping fibers. Relation (18) can then be used in the analytical ablation model.

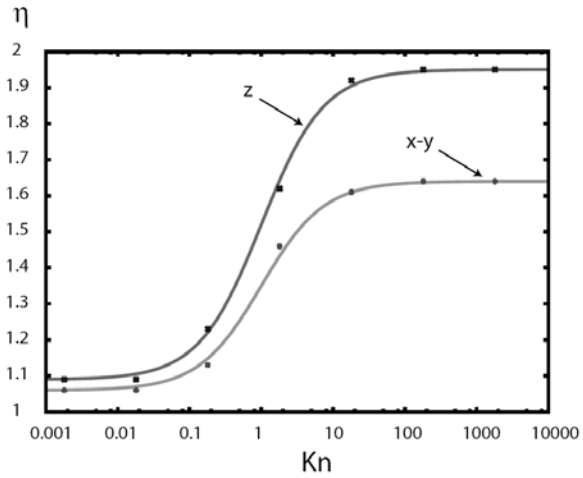

Fig. 8. Tortuosity of the random fibrous medium as a function of Knudsen number, for z and x-y directions (points: DNS; curves: analytical approximations).

APPLICATION TO STARDUST ENTRY ANALYSIS

At peak heating that corresponds to high ablation rate, pressure and temperature are around 10^4Pa and 3000 K, respectively. In these conditions and in air, the mean free path is around 10 µm. The tortuosity in z direction (of interest for the 1D analytical model) is then 1.23. Using Eq. (7), the diffusion coefficient is found to lie around $5 \cdot 10^{-3} m^2/s$. In these conditions, the intrinsic reactivity of carbon fibers to air is known to be of the order of magnitude of 1 m/s [Drawin 1992, Lachaud 2007]. Figure 6 shows that the ablation regime is transitional and close to full volume ablation. The risk of spallation is high under the hypotheses of the model developed in this study. This explains the observation that the char density has been measured lower than expected during post-flight analyses [Stackpoole, 2008].

CONCLUSION

A phenomenological model for the ablation of random fibrous architecture by oxidation has been proposed. The model includes oxidant mass transfer inside the porous medium, heterogeneous reaction, and fiber surface recession. Three-dimensional numerical simulations have been performed and have shown that ablation was controlled by the competition between reaction and diffusion and that it could be either a volume or a surface process. To help in the analysis, a simplified macroscopic model has been derived analytically using volume averaging. Thiele number has been found to be the key dimensionless number. When the reaction rate is fast compared to mass transfer rate (high Thiele number), the oxidant is mostly consumed at the surface and cannot seep through the porous char; in this case, ablation is a surface process. In the converse case (low Thiele number), the oxidant consumption rate being slow, the oxidant concentration becomes homogeneous inside the porous char and ablation occurs in volume. This volume ablation obviously weakens the structure of the material, which is then likely to undergo spallation under the shear stress of the entry flow. In order to feed the analytical model, the effective diffusivities in bulk, transition and Knudsen regime inside the porous medium have been computed by direct numerical simulation using a random walk algorithm. The tortuosity of the material as a function of Knudsen number is shown to follow a Bosanquet-like relation, from which the effective diffusivity can be computed. The model has finally been used to explain post-flight analysis of Stardust TPS ablation during its re-entry on Earth. Under the hypotheses of the model, ablation is found to be in volume at peak heating (corresponding to highe ablation rate). This explains the fact that the density of the material at the surface was lower that expected using surface ablation models. This implies the necessity of developing a full volume ablation model for a reliable design of the Crew Entry Vehicle TPS. This model should include pyrolysis gas advection, full chemistry, and heat transfer.

ACKNOWLEDGEMENTS

This research was supported by an appointment to the NASA Postdoctoral Program at the Ames Research Center, administered by Oak Ridge Associated Universities through a contract with NASA.

NOMENCLATURE

Latin

C oxygen concentration, *mol/m³*
d_p mean pore diameter, m
D diffusion coefficient, m²/s
J molar ablation rate, mol/m²/s
k reactivity, m/s
Kn Knudsen number
Ls sample length, or TPS thickness, m
$\vec{n}$ vector normal to the surface
P pressure, Pa
P_f local fiber perimeter, m
q local molar flux density, mol/m²/s
s volume surface, m²/m³
S_p local horizontal section of a pore, m²
S(x,y,z,t) surface function
T temperature, K
v surface local velocity, m/s

$\bar{v}$ molecular agitation mean velocity, m/s
x,y,z,t space (m) and time (s) coordinates
Greek
ε porosity
η tortuosity
$\bar{\lambda}$ mean free path, m
$\left\langle \xi_j^2 \right\rangle$ mean square displacement in direction j, m
ρ density, kg/m^3
Φ Thiele number
Ω solid molar volume, m^3/mol
Subscripts
B bulk
e, eff effective
f fiber
K Knudsen
ref reference
w wall

REFERENCES

Drawin S., Bacos M. P., Dorvaux J. M., and Lavigne O. (1992):"Oxidation model for carbon-carbon composites", Proc. 4th International Aerospace Planes Conference, Orlando, Florida, AIAA paper 92-210.

Katardjiev I.V., Carter G., Nobes M.J, Berg S., and Blom H.-O. (1994): "Three-dimensional simulation of surface evolution during growth and erosion", J. Vac. Sci. Technol. A 12 (1), pp. 61-68.

Lachaud J., Vignoles G.L., Goyhénèche J.M, and J.F. Epherre (2006): "Ablation in C/C composites: microscopic observations and 3D numerical simulation of surface roughness evolution", Ceram. Trans., Vol.191, 149–160.

Lachaud J., Bertrand N., Vignoles G.L., Bourget G., Rebillat F., Weisbecker P. (2007): "A theoretical/experimental approach to the intrinsic oxidation reactivities of C/C composites and of their components", Carbon, Vol. 45, pp.2768-2776.

Lachaud J., Aspa Y., and Vignoles G. L. (2008): "Analytical modeling of the steady state ablation of a 3D C/C composite", International Journal of Heat and Mass Transfer, Vol 51 (9-10), pp. 2618-2627.

Moyer C. B. and Rindal R. A. (1968): "An analysis of the coupled chemically reacting boundary layer and the charring ablator", NASA CR-1061, 168 p.

Perrins W.T., McKenzie D.R., and McPhedran R.C. (1979): "Transport properties of regular arrays of cylinders", Proc. R. Sod. Lond., A 369, pp. 207-225.

Plapp M. and Karma A.(2000): "Multiscale Finite-Difference-Diffusion-Monte-Carlo method for Simulating Dendritic Solidification", J. Comput. Phys., Vol 165, pp.592-619.

Reid R.C., Prausnitz J.M., and Poling B.E. (1987): "The Properties of Gases and Liquids", fourth ed., McGraw-Hill Book Company, pp. 1–688.

Stackpoole M., Sepka S., Cozmuta I., and Kontinos D. (2008): "Post-flight evaluation of Stardust sample return capsule forebody heatshield material", AIAA-2008-1202, 12 p.

Tomadakis M.M. and Sotirchos S.V. (1993): "Ordinary and transition regime diffusion in random fiber structures", AIChE Journal, Vol. 39, No. 3, pp. 397-412.

Transvalidou F., Sotirchos S.V. (1996): "Effective diffusion coefficients in square arrays of filament bundles." AIChE Journal, Vol. 42, No 9, pp. 2426–38.

Vignoles G.L., Coindreau O., Ahmadi A., and Bernard D. (2007):"Assessment of geometrical and transport properties of a fibrous C/C composite preform as digitized by X-ray computerized microtomography: Part II. Heat and gas transport properties", J. Mater. Res., Vol.20, No 9, pp.1537-1550.